Computational fluid dynamics application to aerospace science

J. S. Shang
joseph.shang@wright.edu
Wright State University
Dayton, Ohio
USA

ABSTRACT

A brief narration on significant accomplishments in computational fluid dynamics (CFD) for basic research and aerospace application is attempted to highlight the outstanding achievements by scientists and engineers of this discipline. To traverse such a vast domain, numerous and excellent contributions to CFD will be unintentionally overlooked by the author's limited exposure. Nevertheless it is an ardent hope that the present abridged literature review will aid to reaffirm excellence in research and to identify knowledge shortfalls both in aerodynamics and its modeling and simulation capability. The future modeling and simulation technology needs, as well as potential and fertile research areas, are humbly put forth for consideration.

1.0 THE EARLY YEARS

In 1933, the first known numerical solution of the Navier-Stokes equations is often attributed to A. Thom who published an article entitled, "The flow past circular cylinder at low speeds" in the Proceeding of the Royal Society of London[1]. However, the most coherent development for computational fluid dynamics (CFD) was initialed in the now Las Alamos National Laboratory (LANL) of United States in the 1940s. This systematic effort was driven by the war-time need for advanced weapon development and from this period of path-finding research, a substantial amount of fundamental knowledge of CFD was generated by J. von Neumann, F. Harlow, C. Hirt, J. Fromm and others. Especially, Von Neumann developed the critical stability criterion for finite-difference approximation and addressed the issue of resolving hydrodynamic shock as early as 1944 and his more accessible article in the literature was published six years later[2,3]. Under the similar war time security restriction, the spherical blast wave computation by G. I. Taylor was also delayed for public release until 1950[4]. These pioneering works were performed to meet an urgent engineering need which set a pattern of science and technology development for practical applications.

Harlow and his colleagues developed the particle in cell(PIC) method based on a combination Lagrangian-Eulerian description of the fluid motion[5]. The PIC method has showed how well suited it was to study time-dependent and multi-dimensional fluid motion. The effectiveness of this method is demonstrated through the applications to shock interaction, supersonic wakes, and hypersonic sharp leading-edge flows. This method is still in use today for Magneto-hydrodynamic research. At the same time, Hirt made a lasting contribution to turbulent transport properties simulation by highlighting the numerical challenges and providing guidance for future research[6]. All these accomplishments were accompanied by exhaustive proof in order to illustrate the validity of the approximations and the numerical accuracy. This rigorous process actually established the standards for all future CFD algorithm and numerical procedure research. The detailed derivation of formulations and extensive discussions on computational accuracy and limits of applicability became the accepted standard in CFD research. During that time, all valuable information was largely unknown to the aerospace science community.

Paper No. 3490. This is the latest in a series of invited survey papers focusing on a specific aspect of the aeronautical industry.

https://doi.org/10.1017/S0001924000003298 Published online by Cambridge University Press

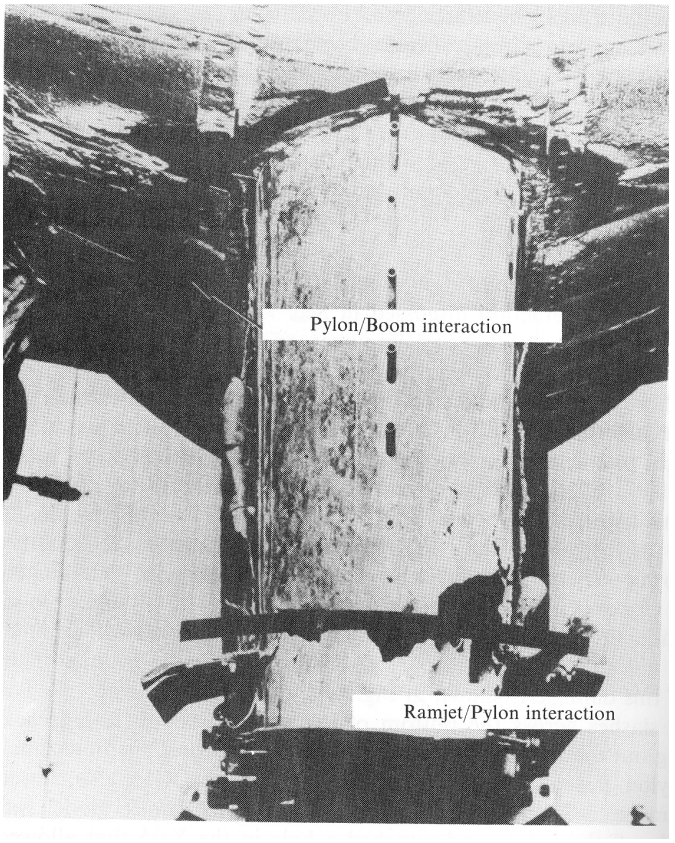


Figure 1. Damaged X-15 ramjet pylon by viscous – inviscid interaction.

Prior to the 1970s, the design and analysis tools in the aerodynamic community were mostly developed from linearised potential flow theory[7], the method of characteristics[8], and boundary-layer theory[9]. In particular, the potential flow methods were routinely used for the aerodynamic performance for aircraft design and analysis. The most widely used tools were the panel methods which have been continually developed and refined over decades[7]. These tools were effective in skillful hands for commercial aircraft design, components of supersonic vehicle evaluation, and thermal management of reentry configuration assessment. However, where analysing aerodynamic performance of high-speed aerospace vehicles is concerned, the shortcoming of these modeling and simulation tools becomes glaring.

An outstanding example of the technical challenge is the evidence of the seriously damaged ramjet pylon and lower surface of the X-15 hypersonic test aircraft by viscous-inviscid interaction that is induced by bow shock impingement as shown in Fig. 1[10]. Several attempts have been made to treat numerically the viscous-inviscid interaction by coupling the pressure gradients of the external flow field to the boundary-layer equations[11]. The scaling laws for both the laminar and turbulent interacting boundary-layer theories were developed based on the concept of K. Stewartson's triple-deck theory[12]. This approach to viscous-inviscid interaction is mathematically elegant and rigorous, but subject to severe limitations for practical application. Finally, it was realised that much greater computational capability for the compressible Navier-Stokes equation must be achieved for any further practical progress.

Meanwhile, a conceptual innovation for solving the inviscid blunt body problem by a time- marching technique was demonstrated by G. Moretti and M. Abett in 1966[13]. Their approach simplifies drastically the computational process for the numerical simulation. By solving the time-dependent Euler equations, the governing differential system becomes hyperbolic. The mixed subsonic and supersonic flow domains can be solved simultaneously. Unlike the traditional solving procedure for steady flow the distinctive regions must be divided into two and treated separately, the need of specifying initial values for the supersonic flowfield downstream to the sonic line is completely eliminated. In fact, the time-marching technique becomes the standard procedure for CFD regardless of whether the solution has a steady state asymptote or not.

2.0 THE 1970s

Two individuals were instrumental in sustaining CFD development for aerodynamic applications in the next three decades; H. Marks was the Director of the NASA Ames Research Center and D. Chapman was the Director of the Aeronautical Science Directorate. Their commitment to mature a new discipline for aeronautical research and application was unshakable, their vision for CFD development was crystalline, and their approach for limited resource distribution by the process of peer review and open debate was exemplary[14]. Their most important contribution beyond science and technology is the tradition of unselfish knowledge sharing and mutual respect in the CFD community. Another remarkable lesson in the management of science and technology development was the clear distinction of science from technology. A very large number of scientists, engineers, and scholars from governmental agencies, industrials, and university worldwide participated in the research activities. A huge number of scientists notably from Japan, Germany, France, Italy, and visiting scholars from the then Soviet Union of Russia made substantial contributions to CFD.

The successful CFD activities quickly expanded to all NASA Science and Technology Centers. The Department of Defense also appreciated the need to develop this aerodynamic modeling and simulation technology. CFD research groups were organised in the Air Force, Army, and Navy Research Laboratories. In order to gain a global competitive edge, CFD research also thrived in the aerospace industries: Boeing, General Dynamics, Lockheed, McDonnell, Douglas, Northorp, and Grumman also established sisable research and development CFD teams. The knowledge transfer path was highly nontraditional at the beginning of CFD development. The knowledge actually flowed from government agencies to academia and industry.

In 1969, R. MacCormack made his breakthrough in numerical algorithm development for solving the compressible Navier-Stokes equations[15]. His explicit, predictor-corrector finite-difference algorithm is simpler than the classic Lax-Wendroff scheme and is much more robust for shock capture by including a pressure damping term. His numerical method became the enabling tool for simulating and understanding the strong viscous-inviscid phenomena. The early work on compression ramp and shock-boundary interactions by C. Hung *et al*[16], J. Shang *et al*[17,18], and C. Horstman *et al*[19] provided a better basic understanding of the boundary-layer separation, and exposed the weakness of rudimentary turbulent closure models. The very few early solutions by solving the Reynolds-averaged Navier-Stokes equations were for shock-boundary-layer interaction including flow separation. In this connection, D. Knight[20] also first applied this numerical technique to simulate realistic high-speed inlets for analysing the performance of air-breathing engines. A sustained research effort in shock-boundary interactions has been maintained for the past fifty years, and recently D. Dolling has summarised all these efforts in an excellent review article[21].

In the late 1970s, even a three-dimensional hypersonic compression corner problem was successfully simulated using MacCormack's explicit method[22,23]. The computational domain of a strong hypersonic shock-boundary-layer interaction was confined in a frustum of a rectangular pyramid by a coarse mesh system of 9,216 points, bounded by a wedge and a flat plate. A physically meaningful solution was obtained by invoking the salient feature

https://doi.org/10.1017/S0001924000003298 Published online by Cambridge University Press

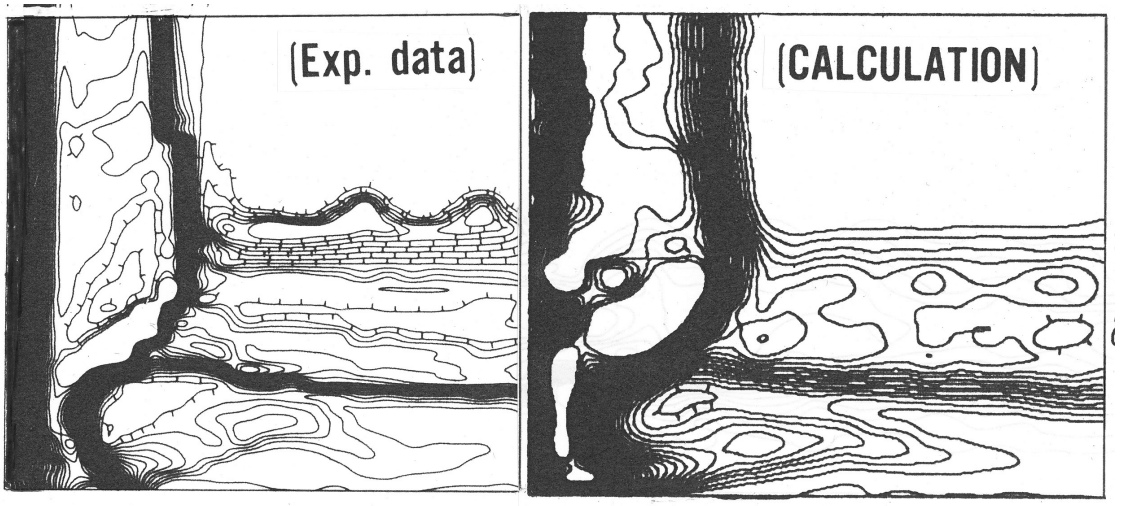


Figure 2. Comparison of trip-point shock structure in hypersonic corner flow.

from the hypersonic equivalence principle – the dominant flow perturbation occurs mostly in the cross flow plane. The numerical results reached impressive agreement with experimental measurements in heat transfer rate and surface pressure distribution. Equally important, the triple-point shock structure was captured at the corner flow region of the wedge and the sharp leading-edge flat plate[22]. From these computational results, the hot spot in the corner region of the X-15 was identified as the penetrating inviscid stream at the shock triple point. The comparison of the simulated and measured shock-wave structure is depicted in Fig. 2 to illustrate the intricate flow structure of viscous-inviscid interaction. Although these types of numerical computations resolved only the essential features of interacting flow fields around mostly rectangular linear configurations, they began to become a powerful tool for aerodynamic basic research.

The body orientated coordinate generation technique introduced by J. Thompson allows CFD to venture into the reign of practical engineering application[24]. His work indeed has opened a new avenue for CFD applications to practical and complex configurations, ahead of any other physics-based simulation discipline. For structured grid computations, the grid can be generated by solving elliptic or hyperbolic partial differential equations, and algebraic equations. The three-dimensional coordinate transformation technique is the cornerstone for CFD application to complex configurations.

A conceptually innovative numerical procedure, by a combination of central and windward difference approximation to satisfy the principle of domain of dependence, was originated by E. Murman and J. Cole[25]. The transonic small disturbance theory was used to solve the flow past thin aerofoils with imbedded shock waves. The mixed elliptic-hyperbolic differential equation was solved by a separate difference formula in the subsonic and supersonic regions to account properly for the local domain of dependence. Their accomplishment again reinforces the fundamental rule in algorithm development – the most accurate and efficient numerical procedure for problem solving is the one that best mimics the physics.

During the same time frame, A. Jameson[26] started to develop an explicit numerical procedure for transonic flows and initiated an illuminative career in CFD. He has made remarkable contributions in developing the shockless transonic wing, multigrid algorithm development, and several ingenious aerodynamic optimising techniques. His numerous contributions to transonic aerofoil and wing designs have no peer and equally impressive is his natural ability in nurturing young talents and bringing out the most creativity from them.

The search for high computing efficiency reflects an impressive creativity in the CFD community. An important factor in applying the implicit scheme to solve the Navier-Stokes equations is alleviating the serious conditional stability constraint inherent to explicit algorithms. The implicit method has been known since the 1950s, and especially the alternative direction implicit (ADI) scheme which reduces the need to invert a three-dimensional matrix into consecutive three one-dimensional matrices[27,28]. The successful application in solving the compressible Navier-Stokes equations was first demonstrated by R. Briley and H. McDonald[29,30], and later but independently by R. Beam and R. Warming[31]. The critical element of the factorised implicit procedure by Beam and Warming is the development of a fourth-order damping procedure to suppress the numerical instability that arises from splitting inviscid and viscous terms of the governing equations. A sustained effort by T. Pulliam and J. Steger has made the three-dimensional ADI scheme applicable to a wide range of engineering problems[32].

Another important step forward in CFD technology is the maturation of the finite-volume formulation. The finite-volume formulation of the macroscopic conservation law is intrinsic in the Eulerian frame of reference. The concept of conservation laws is actually defined for an arbitrary control volume. The variation of dependent variables within the control volume, whether they are mass or components of momentum or internal energy, are balanced by the flux across the control surface of this elementary volume. The basic formulation uses the integral form of the Navier-Stokes equations. The finite-volume formulation rigorously enforces the conservative law both on each elementary cell and for the complete computational domain of the flow field. This formulation is also less susceptible to singular behaviour of an axisymetrical shape than the metrics of coordinate transformation in the finite-difference approximation. The first numerical result of this formulation for the Navier-Stokes equations is attributed to MacCormack and Paullay[33], but it was Rizzi and Inouye who first coined the term finite-volume method[34]. However, the finite-volume method was not widely used until the 1980s.

In the first decade of CFD development, the application to aerodynamics was limited mostly to canonical problems such as the viscous-inviscid interaction over a compression ramp, shock impingement including separated flow[16-19], and three-dimensional corner flows with shock-shock interaction[22,23]. Some previously unsolved problems like bodies at high angle of attack by W. Helliwell *et al* led to a better understanding of the vortical formation in the lee-side of the configuration[35]. Similar path-finding efforts

https://doi.org/10.1017/S0001924000003298 Published online by Cambridge University Press

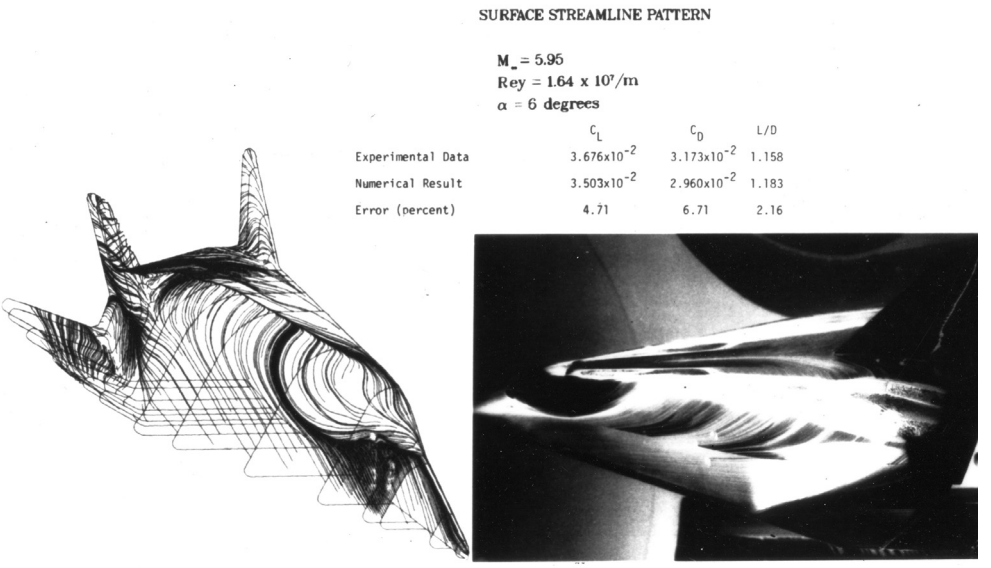


Figure 3. Surface streamline of X-24C.

were also accomplished for the flow structures of unsteady transonic aerofoils by L. Levey[36] and aileron buzzing by J. Steger *et al*[37]. An even more fundamental challenge of examining boundary-layer stability by solving the Navier-Stokes equation was tackled by H. Fasel[38].

3.0 THE 1980s

In the previous decade CFD had been firmly established as a credible tool for aerodynamics research. Significant results were obtained for the inviscid-viscous interactions, including flow separation and flows over arbitrary aerodynamic configurations for a wide range of Reynolds and Mach numbers[39]. Aided by some rather crude and heuristic turbulence models, success was achieved even for complex turbulent flows. In spite of all these convincing demonstrations, the objective of a wide application of CFD in engineering design was yet to be achieved. The basic limitation is imposed by the cost effectiveness of engineering. A lower cost and systematic computational methodology needed to be developed. From the viewpoint of CFD, the obstacles involved several key issues such as; the efficiency of computational algorithms, numerical resolution, automatic grid-point generation, turbulence modeling, and supporting computing facilities. Substantial progress was made in these interlocked problem areas, but continuous efforts were still in demand.

Efforts to develop more efficient finite differencing schemes led to a group of implicit and hybrid procedures[30-32,39]. In general, these attempts were successful and achieved an order of magnitude improvement in computing speed by enhancing the numerical stability. On the other hand, a class of computers designed for scientific computations; the CRAY-1, STAR 100, and ILLIAC IV became available[39-42]. The most significant advance in computer hardware related to CFD at that time was the Cray's vector processor which permitted a vector to be processed at an exceptional high speed. This option gave a new perspective, i.e., a drastic reduction in computing time. Several efforts on vectorisation of computer codes with varying degrees of success have been reported in the open literature[40,41]. The potential of increased speed in data processing rate is clear. Basically, the objective of the vectorisation of a computer code is to construct a long-ordered data string according to the computer structure and to be processed by the vector registers and to achieve optimum data flow.

The performance of a typical three-dimensional Navier-Stokes program on the CRAY-1 computer achieved a data processing rate of 42·9 MFLOPS (million floating point operations per second) in the vector mode which was 127·7 times faster than the rate on a CDC 7600 scalar computer[42]. Meanwhile an approach for solving the approximate Riemann problem for strong shocks was systematically formulated by Roe[43]. Based on these newly gained numerical techniques and computing technology, applications were extended to include missile-like shapes, spinning pointed cones, blunt biconic configurations with and without flaps, and planetary-entry configurations[44-48]. Rapid progress also was made in simulating aerofoil and wing, wing-fuselage, afterbody, wake, propulsion system and combustion, and unsteady phenomena[44]. Various simplifications of the Navier-Stokes equations were also developed, covering a wide range from the paraboloised to the thin-layer approximation according to the problem simulated.

The progress toward simulating aerofoils and wings is particularly noticeable, especially for the complex unsteady aerofoil and two-dimensional leading and trailing edge of lifting surfaces, including flow separation[36,37,44,49]. However, there are only a few solutions of three-dimensional wings known during that time. Usually the solving schemes were approximate procedures to the full Navier-Stokes equations, whether by the conical or parabolised approximation. The slab delta wing at high angle of attack and hypersonic Mach numbers was simulated by Tannehill *et al* using the parabolised Navier-Stokes equations[50]. Their paper also presents an excellent discussion of the departure solution and the treatment of the streamwise pressure gradient. Numerical simulations of blunted delta-wing and strake delta-wing configurations were obtained by Fujii *et al* with the thin-layer approximation[51]. A finite wing (ONERAM6) at transonic Mach number and Reynolds number of 1,000 was also completed by Hollanders *et al*[52].

CFD application also continued its expansion into propulsive systems and combustion. The accomplishments by Anderson[53] for internal flows and scramjet inlet were recorded. The Navier-Stokes equations were also solved in the combustion propulsion system by Kumar[54]. Application in combustion, initiated earlier by Spalding, Pantankar and others[55], was refined by the significant progress in numerical algorithm and computing technology advancement. Combustion in rocket jet plumes and fuel injectors was successfully simulated by Markatos[56] and Drummond *et al*[57]. Novel solutions were obtained for an internal-combustion engine by Griffin *et al*[58] and a chemical laser system[44]. These research efforts revealed a

https://doi.org/10.1017/S0001924000003298 Published online by Cambridge University Press

rapidly growing interdisciplinary thrust of computational aerodynamics in conjunction with chemical kinetics.

The first ever CFD simulation of a complete aerospace vehicle configuration was accomplished in 1986 for X-24C-10D, which is a reentry lifting body of blunt leading edge with canopy, strake, fin, and wing[59]. The series of boost-glide vehicles were adopted for exploring the landing characteristics at low lift-drag ratios and provided a design data base for the Space Shuttle. The numerical solution was obtained at the Mach number of 5·95, a characteristic Reynolds number of $16{\cdot}4 \times 10^6$/m, and at six degrees of angle of attack to duplicate the experimental condition. The numerical result was generated at 120 streamwise stations and by 110 nodes in each cross-flow plane and used a total memory space of 475,200 words. For this computational simulation, the numerically predicted aerodynamic performance data for C_L and C_D are within the wind-tunnel measuring error band of around 6%. The side-by-side comparison of the surface shear flow pattern by numerical simulation and the surface oil flow is presented in Fig. 3 and the lines of scavenging and converging shear flow on the vehicle surface bear closely affinity. As a benchmark, the CFD technique was recognised as a critical technology development for National Aero-space Plane (NASP) and Space Shuttle applications[60,61].

In a relatively short time, the CFD capability was rapidly developed for evaluating aircraft performance. The first aircraft simulation was focused on the fighter F-16A through a close coordination between the Air Force Research Laboratory, NASA Ames Research Center, and General Dynamics[62,63]. The computed surface pressure over the wing, fuselage, and vertical tail agrees very well with the wind-tunnel data obtained at a Mach number of 1·2, Reynolds number of $1{\cdot}275 \times 10^7$, and at a angle of attack of six degrees. The surface shear flow pattern over the lifting surface and wing-fuselage juncture is given in Fig. 4 to show the complex footprint of the rapidly changing external flow field. The validated aerodynamic simulation capability was utilised years later for improving the structural integrity of the wing in dynamic maneuvering. The CFD simulation was also applied to study the vortex breakdown and tail buffet phenomenon of the F-18 fighter[64-66]. This modeling and simulation capability was also used to analyse the structural response to a flexible vertical tail of the F-15 and for advanced fighter aircraft design.

The rapid maturation of CFD for aerospace applications spurred further numerical algorithm innovations. The accomplishments in the high-resolution windward and the total variation diminishing (TVD) schemes by Harten *et al*[67] and Shu[68] are noteworthy and directly usable for application. For high-speed aerodynamics simulation, the nonequilibrium thermodynamic and chemical reaction of high-temperature gas phenomenon must be considered. This thrust CFD into the arena of interdisciplinary computational fluid dynamics, including quantum physics for high-temperature, nonequilibrium, chemical reacting gas phenomena. The work of Candler *et al*[69] exemplified this path-finding research and opened a new research avenue. Meanwhile, the needs of stealth technology and embedded antenna design also inspired a flow of knowledge transfer from CFD to Computational Electromagnetics (CEM) in the time domain. This approach was intended to augment the radar cross section (RCS) prediction from the ray-tracing technique based on optical physics into the time and frequency domain. The interaction between CFD and CEM was sustained into the next decade[70,71].

4.0 1990s

The CFD applications in this decade were dominated by National Aero-Space Plane (NASP) and Space Shuttle. In fact, the aerodynamic design of the space shuttle was initiated as early as the later 1960s and CFD played a relatively minor role in the initial design process. The NASP however, occupied the premier position in CFD

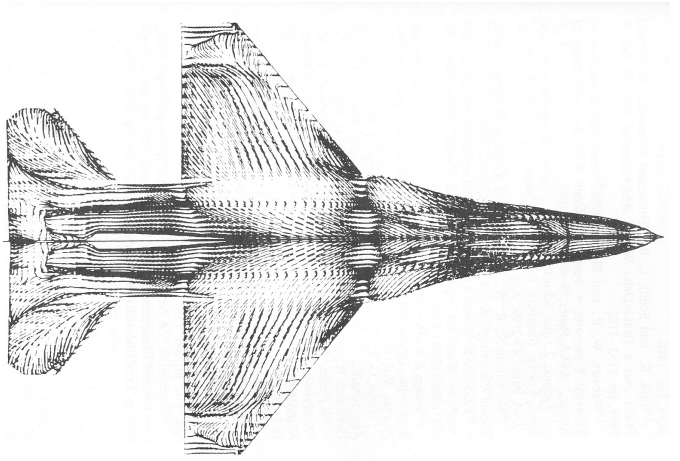


Figure 4. Surface shear pattern of F-16C, M = 1·2, Rey = $1{\cdot}28 \times 10^7$, α = 6 degree.

application to aerospace vehicle design as well as hypersonic flow research and development from 1986 through to 1994. Nearly all sectors of the US aerospace industry, service laboratories of the Department of Defense, national laboratories of the Department of Energy, and more than fourteen major universities actively participated in this program[60].

The goal of the NASP program was to develop and demonstrate the feasibility of a single-stage-to-orbit (SSOT) vehicle that can take off from conventional airfields, accelerate to hypersonic speeds, achieve orbit in a single stage, deliver useful payloads to space, and return to Earth with air-breathing propulsive capabilities. It was and still is a quantum leap from the traditional approaches to aircraft and space vehicle design. The NASP demonstration aircraft, X-30, was to operate through the atmosphere from subsonic speeds to orbital velocities (Mach 25) and accelerate in the atmosphere by a combination of ramjet and scramjet engines. The challenge of developing the high-temperature material for vehicle fabrication was a major issue, but to describe the harsh aerodynamic and thermodynamic environment was a prerequisite. During that time there were no large-scale test facilities to experimentally validate aerodynamic and propulsion operation above Mach 8. Thus the design and analysis of X-30 had to be carried out by CFD alone[72].

The capability for airframe design and flight control/stability was not an overreach, but the required propulsion systems based on subsonic and supersonic ramjet combustion faced, a formidable challenge[73,74]. Especially, the combined cycle engines were only investigated in ground-based facilities and no flight data were available. The critical technology need was the development of a hydrogen-fueled scramjet to operate over the wide speed range from around Mach 4 to 15 and beyond. The NASP program indeed generated an enormous amount of ramjet/scramjet engine research and accelerated the maturation of CFD technology for aerospace application. Many of the detailed achievements still remain classified[74].

The major CFD predictive capability to support NASP applications may be summarised in the aerodynamic simulations based on mass-averaged Navier-Stokes equations, including equilibrium and finite-rate chemical reactions by Walters *et al*[75]. The computer code developed through the NASP program was commercialised to appear as the GASP, and remains even today as a mainstay for high-temperature aerodynamic predictive tool for a wide range of engineering applications. The parabolised Navier-Stokes code for supersonic combustion was developed by Tannehill *et al* to support the NASP[76-78]. This computer code was actually adopted in performing the nose-to-tail analysis for the scramjet propulsive system. A typical calculation using an algebraic turbulence model and a reduced chemical kinetics model on a multiple-zone mesh

https://doi.org/10.1017/S0001924000003298 Published online by Cambridge University Press

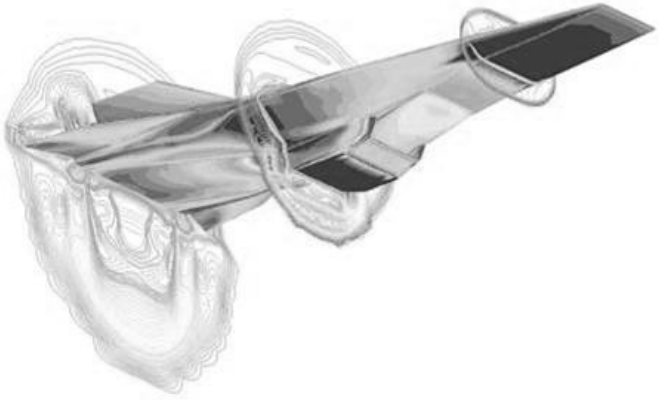


Figure 5. Simulated X-30 in flight.

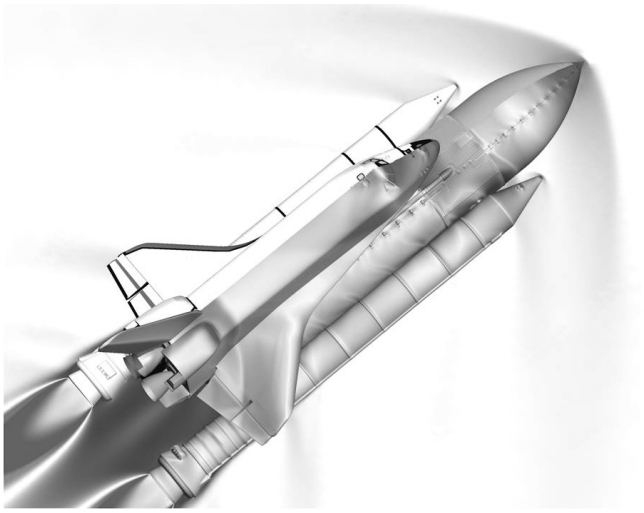


Figure 6. Space Shuttle with detailed surface definition.

system of eight million nodes frequently required about 300 hours computing time on the Cray C-90. The simulated X-30 in flight is presented in Fig. 5 from a scholarly summary of the hypersonic propulsion technology by Drummond *et al*[78]. The NASP was eventually down scope and transformed into the HYFLITE program but a significant amount of mutual support and validation between experimental and CFD had been conducted and hastened the maturation of modeling and simulation technology.

The CFD application to the Space Shuttle accelerated after the Challenger(STS51-L) accident in 1986. A series of computational analyses were initiated to address discrepancies in the design database in regard to both Reynolds number scaling, exhaust-plume-Orbiter interaction, and a complete and more detailed description of the launch vehicle flowfield[61,79,80]. A more stringent accuracy requirement was also imposed to predict the Orbiter wing root shear to within 5% of the maximum structural capability of the wing. To answer this engineering accuracy requirement for a multiple component aerospace system, innovation in grid generation and in data flow between different computational domains were essential.

The simulated Space Shuttle configuration consists of the orbiter, external tanks, plus two solid rocket boosters. The full-scale, high fidelity grid model with many fine geometry details of the Space Shuttle launch vehicle was built using the ICEM/CFD CAD and gridding software. The multiple-zonal grid was smoothed using the GRIDGEN3D software. Finally, 111 grid blocks with a 16 million grid point system were used, and the surface resolution on average was about 10cm[80]. Figure 6 displays the flowfield over the space shuttle in the launching phase; the aerodynamic perturbations induced by the fine-scale structures on the external tank are easily detectable. The earlier numerical solutions for the transonic flow over the vehicle were obtained using the chimera domain decomposition technique[79,80], and then logically transitioned into the unstructured grid method to change how the complex and multi-component configurations were simulated[81].

A less glamorous CFD application to Space Shuttle operations was the main engine (SSME) design. The incompressible viscous flow was solved by the method of pseudo-compressibility, using an implicit approximate-factorisation scheme[82]. Again, a multiple-zone method was used to compute the internal flow in the turnaround duct, fuel bowl, transfer duct, and the race track of the main engine. These types of computational simulations for engineering application achieved good qualitative agreement with experimental data and became a viable design tool for high-compression ratio liquid rocket engines.

The increasing complexity in physics and huge numerical data management for practical applications put a tremendous pressure on obtaining more accurate and efficient numerical algorithms as well as improved computational resources for higher data processing rates and large memory space. However, the first issue in simulating high-speed flows is the description of turbulence, which is strictly an unsteady, three-dimensional, nonlinear phenomenon with a wide range of length scales and frequency spectra. The Kolmogorov scales of turbulent motion needed to be resolved in time and space, are proportional to the inverse square and the inverse three-quarter's power of the Reynolds number based on a characteristic global scale, respectively[83]. For an aircraft simulation at flight conditions by directly solving the Navier-Stokes equations, a mesh of more than quadrillions of points and a data processing rate of hundreds of teraflops (10^{12} floating point operation per second) are needed[84]. Even today's computing resources using distributive memory computer systems are simply unable to meet this requirement economically.

The Application of direct numerical simulation (DNS) to meet engineering needs was, and is still impractical for now, the development of alternatives such as the large-scale eddy simulation method (LES) and further refinement of turbulent modeling becomes necessary[85]. The LES is built upon the premise that the small-scale turbulence is nearly isotropic and has universal characteristics that may be successfully modeled. The large-scale turbulence is resolved by solving the time-averaged Navier-Stokes equations over the fine scale motion and the small-scale turbulence is approximated by some dynamic models[86,87]. The LES technique is successful in addressing the flowfield with additional physical complexities such as combustion and nonequilibrium phenomena. The physical knowledge gained from LES applications has been very beneficial for engineering applications.

It was realised during the 90s that the Nyquist frequency limit for numerical resolution of a wave dominant phenomenon is two discrete points per wavelength, and the numerical process developed from the existing algorithms require at least twenty grid points per wavelength. For any three-dimensional simulation, there is a one thousand fold potential in numerical efficiency improvement[88]. For this reason, high-resolution numerical algorithm development was active, especially the compact differencing formulation. According to Lele[89], the desired feature of a numerical scheme may be derived from optimisation in the Fourier space rather than by focusing on the lowest possible truncation error. In Fig. 7, his assertion is substantiated by the isotropy characteristic of several compact-difference approximations. It reveals that the numerical results of fourth- and six-order accurate algorithms fail to follow the unit circle when the number density per wavelength reduces from the value 16 to 2 in the first to the fourth

https://doi.org/10.1017/S0001924000003298 Published online by Cambridge University Press

quadrant. By adopting the compact differencing algorithm, the improvement in numerical efficiency was realised by a factor more than sixteen times over the most widely adopted second-order scheme, but still fell short of the optimal goal[88].

The LES simulations based upon the compact differencing scheme have been successfully applied to simulate supersonic cavity flow and viscous-inviscid interaction over a compression ramp by Rizzetta *et al*[90,91]. In Fig. 8, the instantaneous Mach number contour at the middle span of a 24-degree compression ramp is displayed. The spatially under-resolved stresses in the large-eddy formulation were accounted for by the Smagorinsky dynamic subgrid model[90]. The comparison with unsteady surface pressure measurements has shown correspondence in distributions of standard deviation, skewness, kurtosis, and intermittency.

The parallel or concurrent computing with shared or distributed memory by a cluster of multiple computers was the solution offered by the computing technology community for generating a high data processing rate. An initiative for multiple-computer development was put forth by the Defense Advance Research Project Agency (DARPA) in conjunction with the Department of Energy (DOE), and became the last major funding effort by government indirectly to advance CFD technology. At the early stage of concurrent multi-computers development, there were a wide range of systems of shared- and distributive- memory computers (Cray T3E, IBM SP, SGI Origin 2000, N-cube etc). Therefore the strategy of porting the most sequential CFD computer codes adopted the domain decomposition approach because it was the most flexible and efficient data partition; it implicitly contained the one- and two-dimension data partitions as subsets[92,93]. The message passing interface (MPI) becomes the mainstay of concurrent computing paradigm, despite the disadvantages of higher cost of computer code development and much less readability and less maintainability than the sequential version. Nevertheless, the standard for parallel computing performance is a straightforward and unattainable superlinear speedup - The factor of speedup of parallel computing is directly proportional to the number of reduced instruction set computers (RISC) in use. During that time, the data processing rate has reached values of more than one GFLOPS (Giga floating point operation per second, 10^9 FLOPS) and the size of distributed memory has approached a terabyte.

The massively parallel computing technology elevates the unstructured grid methodology to a higher level of performance. For large scale computing simulations, the domain decomposition strategy is most efficient when using the message-passing paradigm[92,93]. The redundant data structure for the unstructured grid procedure is actually required for the domain decomposition approach. In addition, the load balancing for efficient parallel computing is nearly automatically achievable to make all unstructured grid procedures scalable. Impressive high parallel numerical simulation efficiency and versatility of unstructured Navier-Stokes/Euler equations solvers has been demonstrated by the work of Strang *et al*[93]. All military aircraft in service or in the design stage such F-22, F-119, B-2 have been simulated for design refinement or performance improvement as shown in Fig. 9. This CFD aerodynamic performance simulational capability for high-lift commercial aircraft was also applied to commercial aircraft design. The most noticeable accomplishments in this aspect were the computations of a Boeing 747 by Cao *et al*[94] and a Boeing 777-200 by Roger *et al*[95]. A dream that one can evaluate the aerodynamic performance of any complete aircraft in a few weeks has been realised over the past thirty years.

The CFD application in Europe has progressed at nearly the same pace as in the United States but with a much stronger emphasis on tool development and a more systematic approach to the validating process. In the late 1990s, a total of nineteen CFD codes in Europe were available for aircraft design and analysis. Among them, fourteen are based on structured grid technology, seven are by unstructured formulations, and the rest are hybrid

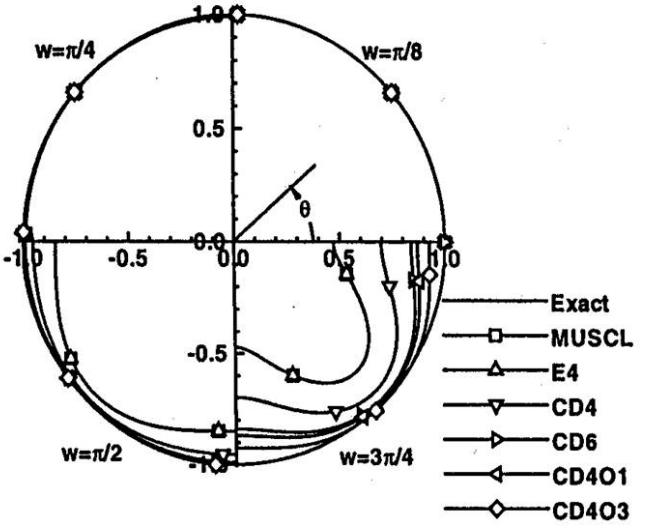


Figure 7. Isotropy characteristic of semi-discrete scheme.

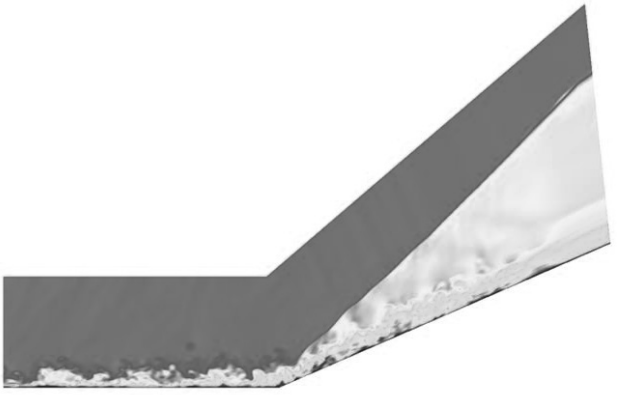


Figure 8. LES application to supersonic compression ramp.

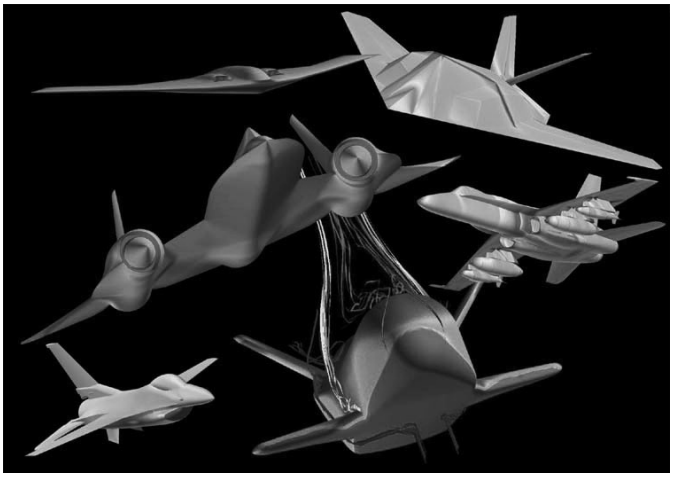


Figure 9. Simulated aerodynamic performance of aerospace vehicles by unstructured grid technique.

https://doi.org/10.1017/S0001924000003298 Published online by Cambridge University Press

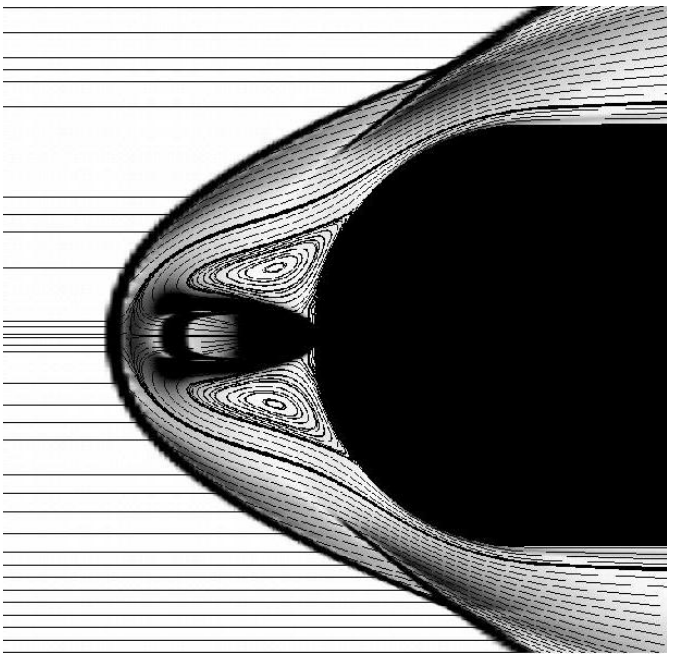


Figure 10. Multiple shocks structure of counter-flowing plasma injection.

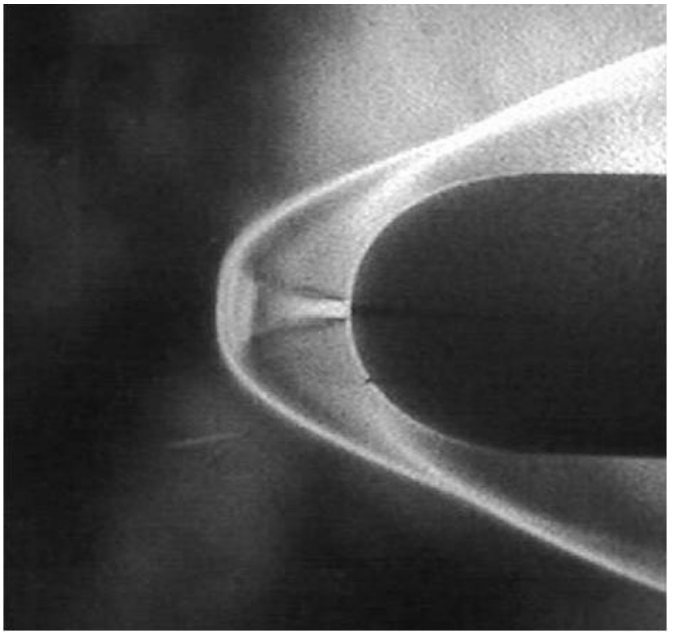


Figure 11. Schlieren photograph of counter-flowing jet injection, $M = 6{\cdot}0$.

versions of the Navier-Stokes Solvers. Some of these activities in computer code development and validation were organised by national aeronautical research establishments in collaboration with the national aeronautical industry and were augmented by the NATO/AGARD (now the NATO/RTO) Fluid Dynamics Panel. The accomplishments are reflected by the successful simulation of the JAS39 Gripen, Eurofighter, Tornado store separation, and the commercial aircraft designs from Falcon 900 to Airbus A380. A comprehensive description can be found in the work of Vos *et al*[96].

5.0 2000s

In the early 2000s, a renewed interest in magneto-aerodynamics research was engendered by the Ajax Program of Russia[97]. This concept vehicle has rejuvenated interest worldwide and offered some opportunities for flow control using electromagnetic forces[98]. Earlier advances were especially noticeable in counter-flow plasma injections for hypersonic flow drag reduction[99,100], plasma actuator for flow control[100-106], a magneto-hydrodynamic (MHD) mechanism for ignition and combustion stability enhancement[107,108], microwave energy deposition for flow field modification[109,110], and a radiatively driven hypersonic wind-tunnel[111]. Although innovative and attractive ideas have been put forward, further development has been inhibited by a limited ability to analyse the extremely complex physics. For example, the concept of magneto-gas-dynamics (MGD) flow bypass for scramjet propulsion is extremely attractive for hypersonic vehicles, but the assessment of these revolutionary concepts remains inconclusive[112,113].

Astonishing amounts of aerodynamic drag reduction via plasma or high-temperature gas injection from the stagnation region of supersonic blunt bodies have been reported in weakly ionised gas research[99]. In the interaction of counter-flow plasma jet and shock, the electromagnetic effects and nonequilibrium thermodynamics were speculated to be the key contributing mechanisms for the drag reduction. However, a combined experimental and computational research effort has revealed the overwhelming portion of wave drag reduction is the result of shock wave degeneration from a single bow wave into a multiple shock structure. The flowfield structure of the counter-flowing plasma injection is depicted in Fig. 10. The Mach disk that terminates the counter-flowing jet and the coalesced ring shock downstream of the reattached shear layer over a three-dimensional recirculating zone can be easily observed from the numerical result. The transition from a single bow shock to the multiple shock structure of the counter-flowing plasma injection has been fully substantiated by experimental observations[100]. The Schlieren photograph presented in Fig.11 made the degenerated shock waves clearly evident. The experiment was conducted at a Mach number of 6·0, a stagnation pressure ratio between the jet and the freestream of 0·75, and the stagnation temperature of the jet at room temperature. Meanwhile the contribution of nonequilibrium thermodynamics and electromagnetic effects in the form of Joule heating associated with plasma injection has been found to be very limited.

In magneto-aerodynamic interactions[98-113], the flow medium needs to be electrically conductive for the introduction of an additional dimension of physics to the fluid motion. Although weakly ionised gas is frequently encountered in hypersonic flow, the ionisation fraction is relatively low, and even for reentry conditions, the electrical conductivity is less than 100mho/m[98]. Therefore, the concentration of charged particles must be enriched for an effective magneto-aerodynamic interaction. It was also realised that a significant plasma-based flow control must be built on a self-sustainable and amplifiable phenomenon that accentuates viscous-inviscid or magneto-aerodynamic interactions. The advantage of using a plasma actuator is obvious; it produces minimum parasitic effect when deactivated and yields huge amount of weight saving in comparison with all traditional flow control mechanisms. For this reason, the plasma actuator became a vibrant technical frontier in the early 2000s.

The effects of Joule heating, electrostatic forces from space charge separation, and Lorentz force from an externally applied magnetic field can be included by integrating the Maxwell and Navier-Stokes equations. For plasma actuator applications, the governing equations are actually an approximation to the classic magneto-hydrodynamics equations for low magnetic Reynolds number[114]. In gist, the Faraday's induction law is dropped from the

https://doi.org/10.1017/S0001924000003298 Published online by Cambridge University Press

governing equations and appends only the Lorentz acceleration to the momentum and the Joule iheating to the conservation of energy equation.

$$\frac{\partial \rho}{\partial t} + \nabla \cdot (\rho \vec{u}) = 0 \quad \ldots (1)$$

$$\frac{\partial \rho \vec{u}}{\partial t} + \nabla \cdot (\rho \vec{u}\vec{u} - \vec{\vec{\tau}}) = \vec{J} \times \vec{B} \quad \ldots (2)$$

$$\frac{\partial \rho e}{\partial t} + \nabla \cdot (\rho e \vec{u} - \vec{q} - \vec{u} \cdot \vec{\vec{\tau}}) = \vec{E} \times \vec{J} \quad \ldots (3)$$

The governing equations are identical to the compressible Navier-Stokes equations except the inhomogeneous terms in the conservation, momentum and energy equations, Equations (1) and (3), include the Lorentz acceleration and the Joule heating, respectively.

Two types of plasma actuators received wide attention. The low-ambient-pressure direct current discharge (DCD) is exclusively adopted for high-altitude hypersonic application[101-103]. The dielectric barrier discharge (DBD) can operate at atmospheric conditions and so is applicable in subsonic and transonic environments[104-106]. The DCD for flow control is built on the effect that the Joule heating decreases local density at the electrodes and creates a sudden growth of the boundary-layer displacement thickness. The altered effective surface slope in turn induces a series of compression waves which coalesce into an oblique shock. The electro magneto-aerodynamic interaction leads to the classic pressure interaction in hypersonic flows[103]. The double-exposure schlieren, Fig. 12, captured this chain of events by a DCD over the flat surface of a wedge in a freestream Mach of 5·15 at the static pressure of 156·2 Pascal with a power input of only 67 Watts.

The DCD actuator has been demonstrated to be a viable flow control mechanism as a virtual leading edge strake[102,103] and a virtual variable area inlet cowl[101,103]. The energy requirement for a DCD flow control plasma actuator is minuscule, 20 watts per centimeter of electrode length but the control effectiveness is also limited to around 10% of the deactivated value. However, the control effectiveness can be doubled or tripled with an externally applied magnetic field, but at the expensive of a substantial complication to the actuator system.

The DBD operates on a self-limiting process in moderating the electric field strength via dielectric surface charge accumulation, and therefore prevents the corona-to-spark transition. The partially ionised gas in the electrode gap is generated through a succession of random streamer formations in space and time. In application, the DBD generally operates at atmospheric pressure, for gap lengths on the order of one millimeter to a few centimeters. An alternative voltage is required to support the random transient streamer formation in the electrode gap and quenching by the localised charge build-up on the dielectric layers[104-106]. In essence, the DBD discharges are operated in the micro-discharge mode and the streamer discharge life cycle is measured in tens of nanoseconds. The complex chemical composition of the weakly ionised gas is fully recognised, but the most profound feature for aerodynamic applications is the charged particles motion over the dielectric barrier. The electro-hydrodynamic interaction through the inelastic collision process between ion and neutral particles produces a wall-jet-like air stream. The maximum magnitude of the wall jet speed can be as high as a few meters per second[104-106]. This energetic wall jet has shown to be very effective for flow control at the aerodynamic bifurcation point such as dynamic stall and laminar-turbulent transition[105].

The plasma generation in DCD and DBD are very similar via the electron collision, secondary surface emission, and the avalanching processes. The dominant mechanisms for the charged particle motion are the electron and ion mobility, and diffusion including

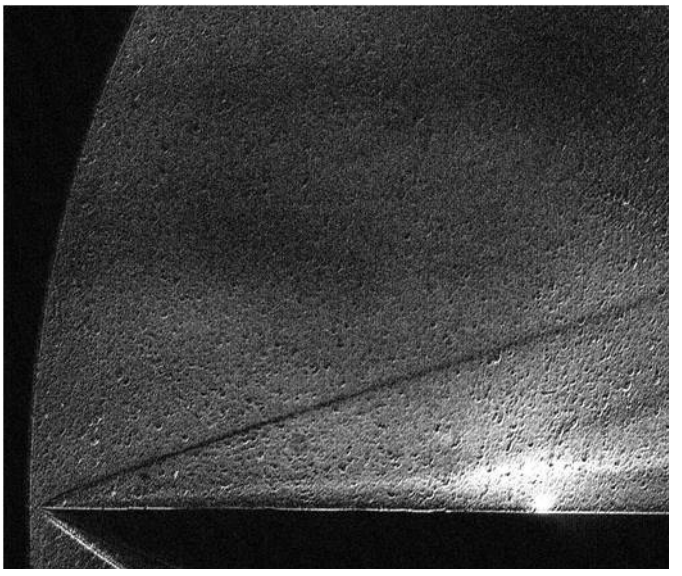


Figure 12. Schlieren of ignited DCD flow control actuator, M = 5·15.

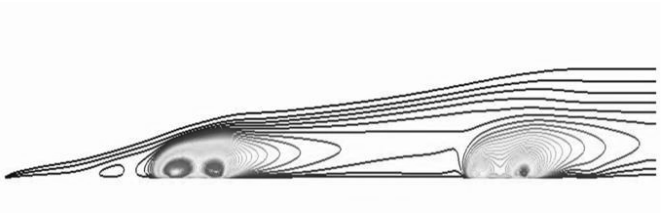


Figure 13. Temperature contours over the discharge electrodes.

the ambiploar diffusion. The classic Townsend formulation is valid[115]. The models of the weakly ionised gas span a range from a relatively simple drift-diffusion theory to a rather elaborate chemical kinetic system[116]. The governing equations of the drift-diffusion model for the three-component plasma (electron, positive charged ion, and neutral particles) can be given as;

$$\frac{\partial n_e}{\partial t} + \nabla \cdot \vec{\Gamma}_e = \alpha(|\vec{E}|, p)|\vec{\Gamma}_e| - \beta n_e n_+ \quad \ldots (4)$$

$$\frac{\partial n_+}{\partial t} + \nabla \cdot \vec{\Gamma}_+ = \alpha(|\vec{E}|, p)|\vec{\Gamma}_e| - \beta n_e n_+ \quad \ldots (5)$$

In the above equations, n_e and n_+ denote the electrons and ions number densities, $\vec{\Gamma}_e = -D_e \nabla n_e - n_e \mu_e \vec{E}$ and $\vec{\Gamma}_+ = -D_+ \nabla n_+ + n_+ \mu_+ \vec{E}$ are the electron and ion density fluxes. In the above formulation, $\alpha(E,p)$ and β are the first Townsend ionisation coefficient and recombination coefficient, respectively. The μ_e and μ_+ are the electron and ion mobility, D_e and D_+ are the electron and ion diffusion coefficients[98,103,115]. The formula for the coefficients of mobility and diffusion is the well-known Einstein relationship[115,117].

The electrodynamic equations for describing the DCD or DBD consist of Equations (4), (5), and the Poisson equation of the plasmadynamics equation. The last equation is derived from the generalised Ampere circuit law and Gauss's law for electric field[115,117]:

$$\nabla^2 \varphi = -\rho_e / \varepsilon \quad \ldots (6)$$

where φ is the electrical field potential and ε is the electrical permittivity. By solving the above equation system, the detailed discharge field over the cathode and anode is given in Fig. 13. The numerical result was generated under the identical condition to duplicate the experimental observation at the Mach number of 5·15

https://doi.org/10.1017/S0001924000003298 Published online by Cambridge University Press

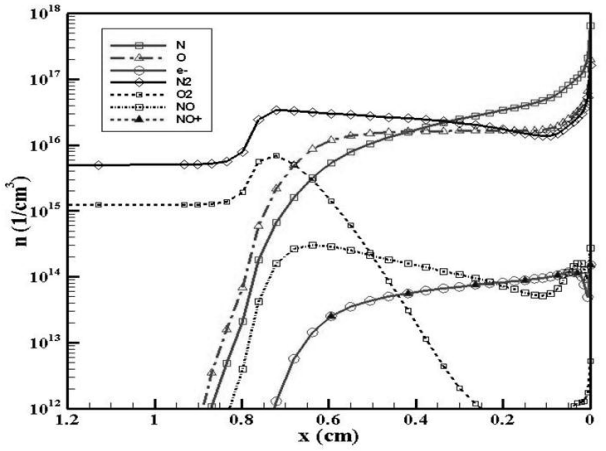


Figure 14. Species concentration along stagnation streamline of RAM-C-II, M_∞ = 23, U_∞ = 7·62kms^{-1}.

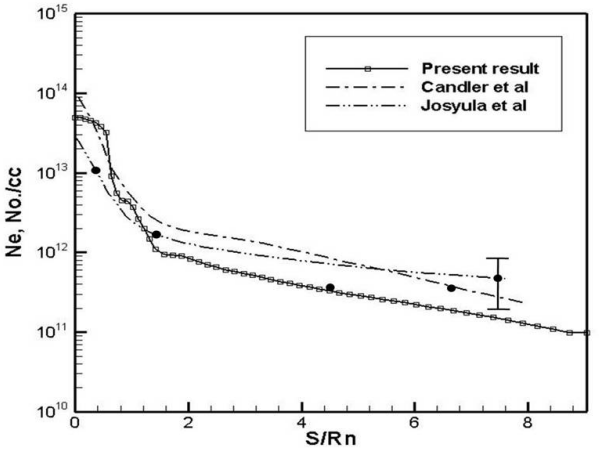


Figure 15. Comparing electron number density distribution along surface of RAM-C-II with flight data

and the static pressure of 156·2 Pascal. The computational result actually shows that the Joule heating is concentrated most over the cathode (left side of the figure) and the intensity is also accentuated over the sharp edges of the electrodes as observed from many experiments.

The plasma actuator development has expanded CFD simulation to include not only electromagnetics but also the high-temperature chemical kinetics and quantum physics. The expanded CFD capability also answered the technical need for increasing interplanetary flight and the earth reentry. For hypersonic entry, the complicated internal degrees of freedom of gas molecules, ablating with surface catalysis, pyrolysis from polymer matrix, and radiation heat transfer must enter consideration. Since the kinetic theory does not consider the internal structure of atoms and molecules, the higher degrees of excitation beyond translation must be modeled by approximations. Traditionally the connection between molecular and atomic structures and the thermodynamic behaviour of high-temperature gas is described by statistical mechanics and augmented by quantum physics. Therefore, the internal degrees of freedom of atomic and molecular species were studied via the partition function and the internal energy transfer was included by separated energy conservation equations[69,118-120].

$$\frac{\partial \rho_i}{\partial t} + \nabla \cdot [\rho_i(\vec{u} + \vec{u}_i)] = \frac{\mathrm{d}w_i}{\mathrm{d}t}, \qquad \ldots (7)$$

$$\frac{\partial \rho u}{\partial t} + \nabla \cdot (\rho \vec{u}\vec{u} + p\vec{\vec{I}} - \vec{\vec{\tau}}) = 0, \qquad \ldots (8)$$

$$\frac{\partial \rho e}{\partial t} + \nabla \cdot [\rho e \vec{u} - \kappa \nabla T + \sum \rho_i u_i h_i + q_{rad} + \vec{u} \cdot p\vec{\vec{I}} + \vec{u} \cdot \vec{\vec{\tau}}] + Q_{vt} - Q_{et} = 0. \qquad \ldots (9)$$

Vibrational energy conservation equation is;

$$\frac{\partial \rho_i e_{iv}}{\partial t} + \nabla \cdot [\rho_i(\vec{u} + \vec{u}_i)e_{iv} + q_{iv})] = e_{iv}\frac{\mathrm{d}w_i}{\mathrm{d}t} + Q_{v,\Sigma}. \qquad \ldots (10)$$

Electronic energy conservation equation can be given as;

$$\frac{\partial \rho_i e_e}{\partial t} + \nabla \cdot [\rho_i(\vec{u} + \vec{u}_i)e_e + \vec{u} \cdot p_e\vec{\vec{I}} + q_e)] = e_e\frac{\mathrm{d}w_i}{\mathrm{d}t} + Q_{e,\Sigma} \qquad \ldots (11)$$

where Q_{vt}, Q_{et}, $Q_{v,\Sigma}$, and $Q_{v,\Sigma}$ are the net energy transfer between translational, vibrational, and electronic excitations. A key addition to the formulation is the rates of energy released from the vibrational-translational and electronic-translational interactions[118-120]. This subject will remain as a sustained research focus into the future and will also extend further to include the effect of ablation.

Modelling of nonequilibrium kinetics has been investigated since the 1930s[118,119], and because all physical-chemical phenomena take place in the molecular and atomic scales for interplanetary reentry application, the finite-rate chemical reaction was modeled on the framework of the Arrhenius equation. The most widely adopted rate constants for high-temperature air are those of Park[120] and those for carbonaceous ablation materials are provided by Park *et al*[121] and Zhluktov *et al*[122]. A substantial amount of research results have been derived from this approach[120-125] and more recently even extended to include the ablation phenomenon[123].

The rate of the species generation and depletion is described by the Arrhenius equation based on the Law of mass action;

$$\frac{dw_i}{dt} = M_i \sum_{j=1}^{J} \left(\nu''_{i,j} - \nu'_{i,j}\right) \left\{ K_{f,j} \prod_{k=1}^{N_{kf}} \left(\frac{\rho_k}{M_k}\right)^{\nu'_{k,j}} - K_{b,j} \prod_{k=1}^{N_{kb}} \left(\frac{\rho_k}{M_k}\right)^{\nu''_{k,j}} \right\} \qquad \ldots (12)$$

The definition of the internal energy is now given as;

$$\rho e = \sum_{i \neq e} \rho_i (c_{v,i} T + \frac{\vec{u} \cdot \vec{u}}{2}) + \sum_{i \neq e} \rho_e e_{v,i} + \sum_{i \neq e} \rho_i h_i^o + \rho_e (c_{v,e} T_e + \frac{\vec{u}_e \cdot \vec{u}_e}{2}) \qquad \ldots (13)$$

where h_i^o is the standard heat of formation for all reacting species. In the absence of an externally applied electrical field, the electron drift velocity vanishes. The driven mechanism for electron motion is solely derived from diffusion, thus the electron velocity can be calculated from Fick's law like all neutral species in the high-temperature gas mixture.

The nonequilibrium hypersonic flow over the Ram-C-II vehicle was often adopted as a benchmark for numerical simulations[69,124,125]. The basic configuration is a spherical cone with a nose radius of 15·24cm and a semi-conical angle of 9 degrees. The overall length of the vehicle is 129·54cm. The flight-test data were collected at altitudes from 53·3 to 85·3km and at flight speed of 7·62kms^{-1} with a small angle-of-attack. Figure 14 depicts the species concentration along the stagnation streamline in particle number density per unit volume. The values of molecular, disso-

https://doi.org/10.1017/S0001924000003298 Published online by Cambridge University Press

ciated, and ionised species including 11 species are included to reveal the complex relaxation phenomena immediately downstream of the bow shock and the classic globally neutral partially ionised plasma behaviour.

However, the most meaningful conclusion can be drawn from the comparison of electron number density measurements in Fig. 15. The major portion of their electron number density data were measured by a reflectometer and a checking point by an electrostatic probe at the distance around eight nose radii from the stagnation point. The estimated error bar of the probe data covers a range of the peak-to-peak density fluctuation from $3{\cdot}0 \times 10^{11}$ to $1{\cdot}2 \times 10^{12}$ per cubic centimeter due the body motion. In this figure all numerical results have reached a reasonable agreement with the flight data although improvement for physical fidelity is still needed.

Renewed studies of important transport properties of the high-temperature gases including dissociating and ionising components have been carried out by Capitelli *et al*[126] and Levin *et al*[127] through collision integrals. Research results from these efforts have reduced the uncertainty in interdisciplinary CFD simulations. A critical research activity for chemical kinetics via fundamental research using an ab initio approach has recently been initiated; the most recent accomplishment is typified in the work by Chaban *et al*[128]. This type of basic research is truly valuable for expanding our knowledge base for the last few frontiers in aerodynamics.

Another CFD application, to micro air vehicles (MAV), is diametrically opposite in flight speed from hypersonic flow. A serious design effort was initiated in 1996 for aircraft as small as possible for special and limited missions that might carry visual, acoustic, chemical, and biological sensors[129]. The required aerodynamic knowledge is significantly different from the traditional and evolutional aircraft design process. Most critical needs are the aerodynamic force and moment evaluation at the Reynolds number as low as a few hundred, and the ability to perform aeroelasticity analysis for deformed lifting components. As the design trend shifts toward flapping wing MAV configurations, the dynamic lift by vortical interaction with a moving surface demands new techniques to simulate flow around rotating and plunging vortex generators with large deformations[130]. On the experimental and flight test aspects, the technique requirement can be met at a much lower scientific threshold. That is we can fabricate and fly test the flapping wing MAV before we fully understand the lifting and maneuvering mechanisms of the associated aerodynamics. Interestingly enough, this technology development is identical to early aircraft design – the experimental simulation leads the theoretical and numerical development.

Again, in order to meet ever increasing accuracy requirements for numerical simulation, several conceptually different approaches were developed. In the later 1990s, the discontinuous Galerkin finite-element method for conservation laws was first introduced to the CFD community by Cockburn *et al*[131]. More recently, the polynomial refinement based on Gauss quadrature which has often been referred to as the spectral difference method, can be considered as an extension from the multi-domain spectral method for unstructured grids[132,133]. The cellwise-staggered polynomial refinement was originated by Korpriva *et al*[134]. In fact, Van den Abeele *et al*[135] have independently showed that the staggered grid multi-domain spectral method and spectral difference methods are independent of how solution points are selected. They also have pointed out the similarities between the spectral based numerical schemes and the discontinuous Galerkin algorithm[131].

The most attractive feature of the polynomial refinement technique is that the procedure is essentially a one-dimensional formulation, and can be equally applicable to spatial and temporal domains. However, the fundamental difference of polynomial refinement from the conventional methods rests on how the approximation is achieved within any arbitrary interval of the real function space. The exact value of the approximated function is ensured at the roots of the orthogonal polynomials through which the accuracy of approximation is uniquely determined by the degree of polynomial[136]. Gauss quadrature employs unequally spaced root or base points, which is diametrically different from the Newton-Cotes formulation for integration. In application, the variables between two temporal or spatial cells can be approximated by any eight known orthogonal polynomials from Legendre to Meixner-Polluckzek, but the former is the mostly widely used because of the accumulative knowledge of this base function. The performance and unique features of polynomial refinement in a steep gradient domain have recently been reasonably established for further research and path-finding applications in combustion and turbulent structures.

7.0 CONCLUDING REMARKS

From the glimpse of the past by a limited exposure in CFD development, one can't but sense that any scientific/technological innovation that enriches our knowledge for human endeavor has always reached farther, and thrived more vigorously, by meeting the need of practical application. CFD as a simulation and modeling tool is still severely limited in its ability for describing physics within the regime of gas kinetic theory. Computational efficiency and accuracy for resolving fine spatial- and temporal-scale aerodynamic bifurcations include laminar-turbulent transition, turbulence, vortex breakdown, and dynamic lift, are still beyond our reach.

In order to accelerate the maturation of this simulation technology for aerospace vehicle design and analysis, research and developmental efforts should be focused on selected topics basic to aerodynamics. Only the technology that builds on the understanding of physical phenomena can further expand the computational capability and attain the widest range of application.

REFERENCES

1. THOM, A. The flow past circular cylinders at low speeds, Proceeding of the Royal Society of London, **A141**, 1933, pp 651-666.
2. VON NEUMANN, J. Proposal and analysis of a numerical method for the treatment of hydrodynamical shock problems, Nat Def and Res Com Rept AM-551, March 1944.
3. VON NEUMANN, J. and RICHTMYER, R.D. A method for the numerical Calculation of hydrodynamic shocks, *J App Phys*, 1950, **21**, pp 232-257.
4. TAYLOR, G.I. The formation of a blast wave by a very intense explosion, *Proc Roy soc London*, Series A, 1950, **201**, pp 159-168.
5. HARLOW, F.H. The particle-in-cell computing method for fluid dynamics, Method in Computational physics, 1964, **3**, p 319.
6. HIRT, C.W. Computer studied of time-dependent turbulent flows, high-speed computing in fluid dynamics, physics of fluid supplement II, *American Inst of phys*, 1969, New York, NY, USA.
7. STRANG, W.Z. BERDAHL, C.H. NUTLEY, E.L. and MURN, A.J. Evaluation of four panel aerodynamic prediction methods (MCAERO, PANAIR, QUANPAN and VSAERO), AIAA-1985-4092, Colorado Springs, CO, USA, 1985.
8. FERRI, A. Application of the method of characteristics to supersonic rotational flow, NACA TN 841, 1946.
9. FAY, J.A. and RIDDELL, F.R. Theory of stagnation point heat transfer in dissociated air, *J Aero Science*, 1958, **25**, pp 73-85 and 121.
10. KORKEGI, R.H. Survey of viscous interaction associated with high Mach number flight, *AIAA J*, 1971, **9**, pp 771-784.
11. LEES, L. and REEVES, B.L. Supersonic separated and reattaching flows: I General theory and application to adiabatic boundary layer/shock wave interactions, *AIAA J*, 1964, **2**, pp 1907-1920.
12. STEWARTSON, K. and WILLIAMS, P.G. Self-induced separation, Proceeding of the Royal Society of London, 1969, **A312**, pp 181-206.
13. MORETTI, G. and ABETT, M. A time-dependent computational method for blunt body flows, *AIAA J*, 1966, **4**, pp 2136-2141.
14. CHAPMAN, D.R. Computational aerodynamics development and outlook, *AIAA J*, 1979, **17**, pp 1293-1313.
15. MACCORMACK, R.W. The effect of viscosity in hypervelocity impact cratering, AIAA 1969-354, Cincinnati, Oh, USA, 1969.

https://doi.org/10.1017/S0001924000003298 Published online by Cambridge University Press

16. HUNG, C.M. and MACCORMACK, R.W. Numerical solutions of supersonic and hypersonic laminar flows over two-dimensional compression corner, AIAA 75-2, 1975.
17. SHANG, J.S. and HANKEY, W.L. Numerical solution of the Navier-Stokes equations for supersonic turbulent flow over a compression ramp, AIAA 75-3, 1975. Also *AIAA J*, 1975, **13**, (10), pp 1368-1374.
18. SHANG, J.S., HANKEY W.L. and LAW, C.H. Numerical simulation of shock wave-turbulent boundary-layer interaction, AIAA 76-0095, 1976. Also *AIAA J*, **14**, (10), October 1976, pp 1451-1457.
19. HORSTMAN, C.C., KUSSOY, M.I., COAKLEY, T.J., RUBESIN, M.N. and MARVIN, J.G. Shock-wave induced turbulent boundary-layer separation at hypersonic speeds, AIAA 75-4, 1975.
20. KNIGHT, D.D. Numerical simulation of realistic high-speed inlets using the Navier-Stokes equations, *AIAA J*, 1977, **15**, pp 1583-1589.
21. DOLLING, D.S. Fifty years of shock/boundary Interaction: What next, *AIAA J*, 2001, **39**, pp 1517-1531.
22. SHANG, J.S. and HANKEY, W.L. Numerical solution of the compressible Navier-Stokes equations for a three-dimensional corner, *AIAA J*, 1977, **15**, pp 1575-1582.
23. SHANG, J.S. and HANKEY, W.L. Three-dimensional supersonic interacting turbulent flow along a corner, *AIAA J*, **17**, 1979, pp 706-713.
24. THOMPSON, J.F., THAMES, F.C. and MASTIN, C.W. Automatic numerical generation of body-fitted curvilinear coordinate system for field containing any number of arbitrary two-dimensional bodies, J Computational Physics, 1974, **15**, pp 299-319.
25. MURMAN, E.M. and COLE, J.D. Calculation of plane steady transonic flows, *AIAA J*, 1971, **9**, pp 114-121.
26. JAMESON, A. Iterative solution of transonic flows over airfoils and wings including flows at Mach 1, *Comm Pure Appl Math*, **17**, 1974, pp 283-309.
27. PEACEMAN, D.W. and RACHFORD, H.H. The numerical solution of parabolic and elliptic differential equations, *J Soc Industrial Applied Math*, 1955, **3**, pp 28-41.
28. DOUGLAS, J. and GUNN, J. A general formulation of alternating direction methods, I, Parabolic and hyperbolic problems, *Numerical Math*, 1964, **6**, pp 428-453.
29. BRILEY, W.R. A Numerical study of laminar separation bubbles using the Navier-Stokes equations, 1971, *J Fluid Mech*, 47, pp 713-736.
30. BRILEY, W.R. and MCDONALD, H. Solution of the three-dimensional compressible Navier-Stokes equations by an implicit technique, Lecture Notes, Phys, **35**, Spring-Verlag, 1974, New York, USA, pp 105-110.
31. BEAM, R.M. and WARMING R.F. An implicit factored scheme for the compressible Navier-Stokes equations, *AIAA J*, 16, 1978, pp 393-401.
32. PULLIAM T.H. and STEGER J.L. Implicit finite difference simulation of three-dimensional compressible flow, *AIAA J*, **18**, (2), 1980, pp 159-167.
33. MACCORMACK, R.W. and PAULLAY, A.J. Computational efficiency achieved by time splitting of finite difference operators, AIAA, pp 72-154, 1972.
34. RIZZI, A. and INOUYE, M. Time-splitting finite-volume method for three-dimensional blunt-body flow, *AIAA J*, **11**, (11), 1973, pp 1478-1485.
35. HELLIWELL, W.S., DICKINSON, R.P. and LUBARD, S.C. Viscous Flow over Arbitrary geometries at high angle of attack, *AIAA J*, **19**, (2), 1981, pp 191-197.
36. LEVY, L.L. Jr Experimental and computational steady and unsteady transonic flows about a thick airfoil, *AIAA J*, **16**, (6), 1978, pp 564-572.
37. STEGER, J.L. and BAILEY, H.E. Calculation of transonic aileron buzz, *AIAA J*, 1980, **18**, (3), pp 249-255.
38. FASEL, H. Investigation of the Instability of Boundary Layers by a finite-difference model of the Navier-Stokes equations, *J Fluid Mech*, 1976, **72**, (2), pp 355-383.
39. LOMAX, H. Recent progress in numerical techniques for flow simulation, *AIAA J*, 1976, **14**, (4), pp 512-528.
40. REDHED, D.D., CHEN, A.W. and HOTOVY, S.G. New approach to the 3D transonic flow analysis using the STAR 100 computer, *AIAA J*, 1979, **17**, pp 98-99.
41. PULLIAM, T.H. and LOMAX, H. Simulation of three-dimensional compressible viscous flow on the ILLIAC IV computer, AIAA Paper 79-0206, 1979.
42. SHANG, J.S., BUNING, P.G., HANKEY, W.L. and WIRTH, M.C. Performance of vectorized three-dimensional Navier-Stokes code on the Cray-1 computer, *AIAA J*, **18**, 1980, pp 1073-1079.
43. ROE, P.L. Approximate Riemann solvers, parameter vectors and difference scheme, *J Comp. Physics*, **43**, 1981, pp 351-372.
44. SHANG, J.S. An assessment of the solutions of the Navier-Stokes equations, *J Aircr*, **22**, 1985, pp 354-370.
45. VIVIAND, H. and GHAZZI, W. Numerical solution of the compressible Navier-Stokes equations at high Reynolds numbers with application to the blunt body problem, Lecture Notes in Physics, **59**, 1976, pp 434-439.
46. PEAKE, D.J., FISHER, D.F. and MCRAE, D.S. Flight, wind tunnel and numerical experiments with a slender cone at incidence, *AIAA J*, **20**, (10), October 1982, pp 1338-1345.
47. AGARWAL, R. and RAKICH, J.V. Supersonic laminar viscous flow past a cone at angle of attack in spinning and coning motion, *AIAA J*, June 1982, **20**, pp 761-768.
48. GNOFFO, P.A. A finite-volume, adaptive grid algorithm applied to planetary entry flow fields, *AIAA J*, **21**, 1983, pp 1249-1254.
49. TASSA, Y. and SANKAR, N.L. Dynamic stall of an oscillating airfoil in turbulent flow using time dependent Navier-Stokes solver, Unsteady Turbulent Shear Flow, Springer-Verlag, New York, USA, 1981, pp 185-196.
50. TANNEHILL, J.C., VENKATAPATHY, E. and RAKICH, J. V. Numerical solution of supersonic viscous flow over blunt delta wings, *AIAA J,* **20**, 1982, pp 203-210.
51. FUJII, K. and KUTLER, P. Numerical simulation of the leading edge separation vortex for a wing and strake-wing configuration, AIAA Paper 83-1908, July 1983.
52. HOLLANDERS, H., LERAT, A. and PEYRET, R. 3D calculation of transonic viscous flows by an implicit method, AIAA Paper 1983-1953, July 1983.
53. ANDERSON, O.L. Calculation of internal viscous flows in axisymmetric ducts at moderate to high Reynolds numbers, *Int J Computers and Fluids*, **8**, 1980, pp 391-411.
54. KUMAR, A. Two-dimensional analysis of a scramjet inlet flowfield, *AIAA J*, **20**, (1), January 1982, pp 96-97.
55. PATANKAR, S.V., PRATAP, V.S. AND SPALDING, D.B. Prediction of laminar flow and heat transfer in helically wield Pipes, *J Fluid Mechanics*, **62**, 1974, pp 539-551.
56. MARKATOS, N.C., SPALDING, D.B., TATCHELL, D.G. and MACE, A.C.H. Flow and combustion in the base-wall region of a rocket exhaust plume, *Combustion Science and Technology*, 1982, **28**, pp 15-29.
57. WEIDNER, E.H. and DRUMMOND, J.P. Numerical study of a staged fuel injection for supersonic combustion, *AIAA J*, **20**, (10), October 1982, pp 1426-1427.
58. GRIFFIN, M.D., ANDERSON, J.D. JR. and DIWAKER, R. Navier-Stokes solutions of the flowfield in an internal combustion engine, *AIAA J*, December 1976, **14**, (12), pp 1665-1666.
59. SHANG, J.S. and SCHERR, S.J. Navier-Stokes solution for a complete re-entry configuration, *J Aircr*, 1986, **23**, pp 881-888.
60. BARTHELEMY, R.R. The National Aero-Space Plane program, AIAA 1989-5053, July 1989.
61. GOMEZ, R., VICKER, D., ROGERS, S.E., AFTOSMIS, M.J., CHAN, W.M. MEAKIN, R. and MURMAN, S.M, STS-107 Investigation ascent CFD support, AIAA 2004-2226, 2004.
62. REZNICK, S.G. and FLORES, J. Strake-generated vortex interactions for a fighter-like configuration, AIAA 87-0589; also, *J Aircr*, **26**, 1989, pp 289-294.
63. HUBAND, G.W., RIZZETTA, D.P. and SHANG, J.S. Numerical solution of the Navier-Stokes equation for an F-16A configuration, AIAA 1988-2057; also *J Aircr*, **26**, 1989, pp 634-640.
64. THOMAS, J.L., WALTERS, R.W., REU, T., GHAFFARI, F., WESTON, R.P. and LUCKRING, J.M. Application of a patched-grid algorithm to the F/A-18 forebody-leading-edge extension configuration, *J Aircr*, **27**, 1990, pp 749-756.
65. SCHIFF, L.B., CUMMINGS, R.M, SORENSON, R.L. and RIZK, Y.M. Numerical simulation of high-incidence flow over the F-18 fuselage forebody, AIAA 1989-0339, 1989 ; also Numerical simulation of high-incidence flow over the isolated F-18 fuselage forebody, *J Aircr*, **28**, 1991, pp 609-617.
66. RIZK, Y.M. and GEE, K. Unsteady simulation of viscous flowfield around F-18 Aircraft at large incidence, *J Aircr*, **29**, 1992, pp 986-992.
67. HARTEN, A., EGQUIST, B., OSHER, S. and CHAKRAVARTHY, S., Uniformly high-order essentially non-oscillatory schemes III, *J Comp Phys*, **71**, 1987, pp 231-257.
68. SHU, C.W. Total –variation-diminishing time discretizations, SIAM *J Sci Stat, Comput.* **9**, 1988, pp 1073-1084.
69. CANDLER, G.V. and MACCORMACK, R.W. Computation of weakly ionized hypersonic flows in thermochemical nonequilibrium, *J Thermophysics*, **5**, 1991, pp 266-273.

https://doi.org/10.1017/S0001924000003298 Published online by Cambridge University Press

70. SHANKAR, V., HALL, W.F. and MOHAMMADIAN, A.H. A time-domain differential solver for electromagnetic scattering problems, Proceedings of Institute of Electrical and Electronics Engineers, 1989, **77**, p 709.
71. SHANG, J.S. Characteristic-based algorithms for solving the Maxwell equations in the time domain, *IEEE Antennas and Propagation Magazine*, **37**, June 1995, pp 15-25.
72. MCCLINTON, C., BITTNER, R. and KAMATH, P. CFD support to NASP design, AIAA 90-5249, October 1990.
73. CURRAN, E.T., HEISER, W.H. and PRATT, D.T. Fluid phenomena in scramjet combustion systems, *Annul Rev Fluid Mech*, 1966, pp 323-360.
74. CURRAN, E.T. Scramjet Engines: The first forty years, *J Propulsion and Power*, **17**, 2001, pp 1138-1148.
75. WALTERS, R.W., CINNELLA, P., SLACK, D.C. and HALT, D. Characteristic based algorithms for Flows in thermochemical nonequilibrium supersonic combustion fields, *A1AA J*, 1992, **30**, pp 1304-1313.
76. TANNEHILL, J. C., BUELOW, P. E., LEVALTS, J. O. and LAWRENCE, S. L. three-dimensional upwind parabolized Navier-Stokes code for real gas flows, *J Spacecraft and Rockets*, **27**, 1990, pp 150-159.
77. WADAWADIGI, G., TANNEHILL, J.C., BUELOW, P.E. and LAWRENCE, S. Three-dimensional upwind parabolized Navier-Stokes code for supersonic combustion fields, *J Thermophysics and Heat Transfer*, **7**, 1993, pp 661-667.
78. DRUMMOND, J.P. and BOUCHE, M. Overview of NATO Background on Scramjet Technologies, 2, Technologies for Propelled Hypersonic Flight, Chapter 1, NATAO-RTO-TR-AVT-007, 2006.
79. BUNING, P.G., PARKS, S.J., CHAN, W.M. and RENZE, K.J. Application of the Chimera overlapped grid scheme to simulation of space shuttle accent flows, Proceedings of the 4th international Symposium on CFD, Davis, CA, USA, 1991.
80. SOTNICK, J.P., KANDULA, M. and BUNING, P. Navier-Stokes simulation of the space shuttle launch vehicle flight transonic flowfield using a large scale chimera grid system, AIAA 1994-1860, June 1994.
81. CHAKRAVARTHY, S.R., SZEMA, K.Y. and CHEN C.L. An universe-series code for inviscid CFD with Space Shuttle applications using unstructured grids, AIAA 1991-3340, 1991.
82. YANG, R.J., CHANG, J.L.C. and KWAK, D. Navier-Stokes flow simulation of the space shuttle main engine hot gas manifold, *J Spacecraft and Rocket*, 1992, **29**, pp 253-262.
83. FRIEDLANDER, S.K. and TOPPER, L. (Eds) Classic Paper on Statistical Theory, *Interscience*, 1962, New York, USA, p 186.
84. SHANG, J.S. Assessment of technology for aircraft development, *J Aircr*, **32**, 1995, pp 611-617.
85. BRADSHAW, P. Turbulence: The chief outstanding difficulty of our subject, *Experimental in Fluids*, 1994, 16 Nos ¾, pp 203-216.
86. CLARK, R.A., FERZIGER, J.H. and REYNOLDS, W.C. Evaluation of subgrid scale models using an accurately simulated turbulent flow, *J Fluid Mechanics*, 1979, **91**, (1).
87. PIOMELLI, U. Large-eddy simulation: achievement and challenges, *Progress in Aerospace Sciences*, **35**, 1999, pp 335-362.
88. GAITONDE, D.V. and SHANG, J.S. Optimized compact-difference-based finite-volume solvers for linear wave phenomenon, *JCP*, **138**, 1997, pp 617-643.
89. LELE, S.K. Finite difference schemes with spectral-like resolution, *J Comp. Phys*, 1992, **103**, pp 16-14.
90. RIZZETTA, D.P. and VISBAL, M.R. Application of large eddy simulation to supersonic compression ramps, *AIAA J*, **40**, 2002, pp 1574-1581.
91. RIZZETTA, D.P. and VISBAL, M.R. Large eddy simulation of supersonic cavity flowfield including flow control, *AIAA J*, 2003, **41**, pp 1452-1462.
92. SHANG, J.S., WAGNER, M., PAN, Y. and BLAKE D.C. Strategies for adopting FVTD on mutlicomputers, *Computing in Science and Engineering*, 2000, **2**, pp 10-21.
93. STRANG, W.Z., TOMARO, R.F. and GRISMER, M.J. The defining methods of Cobalt: A parallel, implicit, unstructured Euler/Navier-Stokes flow solver, AIAA 99-0786, January 1999.
94. CAO, H.V. and SU, T.Y. Navier–Stokes analyses of a 747 high-lift configuration. AIAA Paper, 98-2623, 1998.
95. ROGERS, S.E., ROTH, K., CAO, H.V. SLOTNICK, J.P, WHITLOCK, M., NASH, S.M. and BAKER, M.D. Computation of viscous flow for a Boeing 777 aircraft in landing configuration, 2001, *J Aircr*, **48**, pp 1060–1068.
96. VOS, S.B., RIZZI, A., DARRACQ, D. and HIRSHEL, E.H. Navier-Stokes solvers in european aircraft design, *Progress in Aerospace Sciences*, **38**, 2003, pp 601-697.
97. FRAISHTADT, V.L., KURANOV, A.L. and SHEIKIN, E.G. Use of MHD systems in hypersonic aircraft, *Technical Physics*, **11**, 1998, p 1309.
98. SHANG, J.S. Recent research in magneto-aerodynamics, *Progress in Aerospace Science*, 2001, **37**, pp 1-20.
99. GANIEV, Y. GORDEEV, V, KRASILNIKOV, A, LAGUTIN, V., OTMENNIKOV, V. and PANASENKO, Aerodynamic drag reduction by plasma and hot-gas injection, *J Thermophysics and Heat Transfer*, **14**, 2000, pp 10-17.
100. SHANG, J.S. Plasma injection for hypersonic blunt body drag reduction, *AIAA J*, 2002, **40**, (6), pp 1178-1186.
101. MACHERET, S.O., SHNEIDER, M.N. and MILES, R.B. Magneto-hydrodynamic and electro-hydrodynamic control of hypersonic flows of weakly ionized plasma, *AIAA J*, **42**, 2004, pp 1378-1387.
102. KIMMEL, R., HAYES, J., MENART, J. and SHANG, J.S. Effect of magnetic fields on surface plasma discharges at Mach 5, *J Spacecraft and Rocket*, 2006, **43**, pp 1340-1346.
103. SHANG, J.S., SURZHIKOV, S.T., KIMMEL, R.L., GAITONDE, D.V., MENART, J.A. and HAYES, J.R. Mechanisms of plasma actuator for hypersonic flow control, *Progress in Aerospace Sciences*, 2005, **41**, (8), pp 642–668.
104. LEGER, L., MOREAU E. and TOUCHARD, G. Effect of a DC corona electrical discharge on the airflow along a flat plate, 2002, *IEEE Trans Indust Appl*, **38**, pp 1478-85.
105. POST M.L. and CORKE, T.C. Separation control on high angle-of-attack airfoil using plasma actuator, *AIAA J*, 2004, **42**, (2), pp 2177-2184.
106. MOREAU, E. Airflow Control by non-thermal plasma actuators, *J Physics D: App Physics*, 2007, **40**, pp 605-636.
107. JACOBSEN, L.S., CARTER, C.D. and JACKSON, T.A. Toward plasma-assisted ignition in scramjets, AIAA 2003-0871, Reno, NV, USA, January 2003.
108. ANIKIN, N., KUKAEV, E., STARIKOVSKAIA, S. and STARIKOVSKII, A. Ignition of hydrogen-air and methane-air mixtures at low temperatures by nanosecond high voltage discharge, AIAA 2004-0833, Reno, NV, USA, January 2004.
109. KOLESNICHENKO, Y. Basics in beams mw energy deposition for flow/flight control, AIAA 2004-0669, Reno NV, January 2004.
110. ADELGREN, R.G., YAN, H., ELLIOTS, G.S., KNIGHT, D.D., BEUTNER, T.J. and ZHETOVODOV, A.Z. Control of Edney IV interaction by pulsed energy deposition, *AIAA J*, 2005, **43**, pp 256-269.
111. MILES, R.B., BROWN, G.L., LEMPERT, W.R., YETTER, R., WILLIAMS, G.L., BOGDONOFF, S.M., NATELSON, D. and GUEST, J.R. Radiatively driven hypersonic wind tunnel, *AIAA J*, **33**, (8), 1995, pp 1463-1470.
112. PARK, C., MEHTA, U.B. and BOGDANOFF, D.W. MHD energy bypass scramjet performance with real gas effects, *J Propulsion and power*, **19**, (5), 2001, pp 1049-1057.
113. GAITONDE, D.V. Three-dimensional flow-through scramjet simulation with MGD energy-bypass, AIAA 2003-0172, January 2003.
114. MITCHNER, M. and KRUGER, C.H. *Partially Ionized Gas*, John Wiley & Sons, 1973, New York, USA.
115. SURZHIKOV, S.T. and SHANG, J.S. Two-component plasma model for two-dimensional glow discharge in magnetic field, *Comp Physics*, **199**, September 2004, pp 437-464.
116. SOLOV'EV, V.R., KONCHAKOV A.M., KRIVTSOV, V.M. and ALEKSANDROV, N.L. Numerical simulation of a surface barrier discharge in air, *Plasma Phy Rept*, **7**, (7), 2008, pp 594-608.
117. SHANG, J.S., HUANG, P.G., YAN, H. and SURZHIKOV, S.T. Computational simulation of direct current discharge, *J Applied Physics*, **105**, 2009, pp 023303-1-14.
118. LANDAU, L. and TELLER, E. Zur theore der schalldispersion, *Physik Z. Sowjetunion*, b. 10, h. 1, 1936, p 34.
119. TREANOR, C.E. and MARRONE, P.V. Effect of dissociation on the rate of vibrational relaxation, *Physics of Fluids*, **5**, (9), 1962, pp 1022-1026.
120. PARK, C. Chemical-kinetic parameters of hypersonic earth entry, *J Thermophysics and heat Transfer*, 2001, **15**, (1), pp 76-90.
121. PARK, C. Stagnation-point ablation of carbonaceous flat disk, Part 1: Theory, *AIAA J*, 1983, **21**, (1), pp 1588-1594.
122. ZHLUKTOV, S. and ABE, T. Viscous shock-layer simulation of air flow past ablating blunt body with carbon surface, *J Thermo-Physics and Heat Transfer*, **13**, (1), 1999, pp 50-59.
123. CHEN, Y.K. and MILO, F.S. Navier-Stokes Solutions with finite rate ablation for planetary mission earth mission earth reentries, *J Spacecraft and Rockets*, 2005, **42**, (6), pp 961-970.
124. JOSYULA, E. and BAILEY, W.F. Governing equations for weakly ionized plasma flow field of aerospace vehicles, *J Spacecraft and Rockets*, **40**, (6), 2003, pp 845-857.
125. SHANG, J.S., SURZHIKOV, S.T. and YAN, H. Simulate Hypersonic Nonequlibrium Flow Using Kinetic Models, AIAA 2009-0386, Orlando, FL, USA, January 2009.

https://doi.org/10.1017/S0001924000003298 Published online by Cambridge University Press

126. CAPITELLI, M., GORSE, C. AND LONGO, S. and GIORDANO, D. Collision integrals of high-temperature air species, *J Theromphysics and Heat Transfer*, **14**, 2000, pp 259-268.
127. LEVIN, E. and WRIGHT, M.J. Collision integrals for ion-neutral interactions of nitrogen and oxygen, *J Thermophysics and Heat Transfer*, **18**, (1), 2004, pp 143-147.
128. CHABAN, G., JAFFE, R., SCHWENKE, D.W. and HUO, W. Dissociation cross sections and rate coefficients for nitrogen from accurate theoretical calculations, AIAA 2008-1209, Reno, NV, USA, January 2008.
129. MUELLER, T.J., KELLOGG J.C., IFJU, G.I. and SHKARAYEV, S.V. Introduction to the design of fixed-wing micro air vehicles including three cases studies, AIAA Education Series, Reston, VA, USA, 2006.
130. BERMAN, G.J. and WANG, Z.J. Energy-minimizing kinematics in hovering insect flight, *J Fluid Mech*, 2007, **582**, pp 153-168.
131. COCKBURN, B. and SHU, C.W. TVB Runge-Kutta local projection discontinuous Galerkin Finite element method for conservation laws 2: General frame work, *Mathematics of Comp*, 1989, 52, pp 411-435.
132. WANG, Z.J. Spectral finite Volume method for conservative laws on unstructured grids: basic formulation, *J Comp physics*, 2002, **178**, pp 210-251.
133. LIU, Y., VINOKUR, M. and WANG Z.J. Spectral difference method for unstructured grids I: basic formulation, *J Comp physics*, 2006, **216**, pp 780-801.
134. KORPRIVA, D. and KOLIAS, J. A conservative Staggered-grid Chebyshev multidomain method for compressible flows, *J Comp. Physics*, 1996, **125**, pp 244-261.
135. VAN DEN ABEELE, K. LACOR, C. and Z.J. WANG, On the stability and accuracy of the spectral Difference Method, *J Scientific Computing*, 2008, **37**, pp 162-188.
136. GAUTSCHE, W. Orthogonal polynomials, computational and approximation, Oxford Science Publications, Oxford University Press, Oxford, UK, 2004.

https://doi.org/10.1017/S0001924000003298 Published online by Cambridge University Press